NANO LETTERS

2004
Vol. 4, No. 12
2323−2330

Bioconjugates of CdTe Nanowires and Au Nanoparticles: Plasmon−Exciton Interactions, Luminescence Enhancement, and Collective Effects

Jaebeom Lee,[†] Alexander O. Govorov,[‡] John Dulka,[‡] and Nicholas A. Kotov*,[†]

Department of Chemical Engineering, Department of Materials Science and Engineering and Department of Biomedical Engineering, University of Michigan, Ann Arbor, Michigan 48109, and Department of Physics and Astronomy, Ohio University, Athens, Ohio 45701

Received August 16, 2004; Revised Manuscript Received October 12, 2004

ABSTRACT

Nanoscale superstructures made from CdTe nanowires (NWs) and metal nanoparticles (NPs) are prepared via bioconjugation reactions. Prototypical biomolecules, such as D-biotin and streptavidin pair, were utilized to connect NPs and NWs in solution. It was found that Au NPs form a dense shell around a CdTe NW. The superstructure demonstrated unusual optical effects related to the long-distance interaction of the semiconductor and noble metal nanocolloids. The NW–NP complex showed 5-fold enhancement of luminescence intensity and a blue shift of the emission peak as compared to unconjugated NW. The system was theoretically examined in a simple model of CdTe NW coaxially surrounded by an Au shell, which gives excellent agreement with experimental data. The combination of time-resolved luminescence and calculations demonstrated that increase of fluorescence intensity occurs due to stimulation of photon emission by an electromagnetic field generated around the Au NP. The process is reminiscent of SERS, although displaying smaller enhancement factors. Importantly, the luminescence enhancement should be treated as a collective response of Au–NPs, rather than a result of isolated NP–NW interactions.

1. Introduction. Hybrid self-assembled superstructures made of biological and abiotic nanoscale components present versatile molecular constructs with an array of unique electronic and surface properties.[1−8] Virtually any combination of nanoscale building blocks can be assembled in fascinating one-, two-, and three-dimensional assemblies following this approach.[9−16] Now the question is what kind of functionalities one wants to impart to the nanobiological assemblies. Extensive studies are underway aimed at the utilization of simple nanoparticle−biomolecule conjugates for the monitoring of cells and cell components and for the use of these constructs for biosensing, drug delivery,[17] in-vivo and ex-vivo imaging, cancer treatment, and diagnostics.[18−25] Interesting possibilities are also opening with regard to the biological implants made from nanostructured materials.[26] In addition to the research venues in life sciences, there exists a theoretical possibility that complex and highly organized electronic structures with applications in nanoelectronics and nanophotonics can be self-assembled from biologically connected nanocolloids, similarly to the living cell components. While one should approach the practical prospects of this idea with some dose of skepticism, it should not slow the studies of the optical and electronic interactions of nanocolloids in these superstructures. Multidimensional constructs made of diverse building blocks including metal, semiconductor nanoparticles (NPs), nanowires (NWs)[27−31] and possibly other components are likely to demonstrate a fascinating assortment of electronic properties and cooperative interactions that are fundamentally important for the field of nanotechnology.

Here, we present the first study on the biologically inspired superstructures made from metal NPs and semiconductor NWs, which demonstrate remarkable optical effects stemming from collective interactions of NPs and NWs. A variety of Au and Ag NPs of different diameters with numerous surface functionalities can be easily synthesized in liquid media.[32,33] Optical effects in noble metal NPs, such as surface plasmon resonance, have received a lot of attention over the course of past 15 years. Surface enhanced Raman scattering (SERS)[24,34−36] and related optical phenomena observed in these NPs have been considered an enabling technology for highly compacted optoelectronic devices and sensors which take advantage of both quantum confinement effects and nonlinear optical properties.[37,38]

* Corresponding author. E-mail: kotov@umich.edu
[†] University of Michigan.
[‡] Ohio University.

10.1021/nl048669h CCC: $27.50
Published on Web 11/03/2004

Superstructures from NPs and NWs should still be considered virtually virgin territory of nanotechnology, although a few examples of assemblies of some one-dimensional nanostructures and NPs have been reported. Most attention has been given to the combination of NPs and carbon nanotubes.[39−43] It started when Ajayan et al. showed that carbon nanotubes can be filled with metal resulting in NP/nanotube complexes.[44] Osterloh et al. studied the assembly of CdSe and Au NPs on the surface of $LiMo_3Se_3$ NWs upon the hydrophobic interaction and found that the optical and electronic properties of NPs were largely altered.[45] Penner et al. investigated the "cross-talk" in the nanoconstructs of metal NPs and metal NWs by two-step electrodeposition.[46] Bio-inspired methods of structural design[16,47−49] make the preparation of NP−NW superstructures simpler, faster, more controllable, and versatile.

In this paper, complexes of CdTe NWs with Au NPs have been prepared by taking advantage of a biotin−streptavidin affinity pair. A strong enhancement of fluorescence of CdTe−NWs conjugated with Au−NPs is experimentally demonstrated and theoretically explained. One of the fundamentally relevant features of these superstructures is that the interactions of plasmons in NPs layered on NW have a collective character.

2. Experimental Section. $Cd(ClO_4)_2 \cdot H_2O$, L-cysteine, Al_2Te_3, and NaOH were purchased from Aldrich and used without further purification. Condensed H_2SO_4 was provided from EM Inc. and diluted 0.5 M using 18 MΩ deionized water (Barnstead E-pure system). Streptavidin (SA) and D-biotin (B) were obtained from Aldrich. 1-Ethyl-3-(3-dimethlamino propyl) carbodiimide hydrochloride (EDC) and *N*-hydroxy-sulfosuccinimide (NHS) were purchased from Aldrich and Merck for bioconjugation, respectively. $HS(CH_2)_2CH_3$ and $HS(CH_2)_2COOH$ from Aldrich were employed for bioconjugation of Au NPs.

CdTe NPs and NWs were prepared as mentioned elsewhere in detail.[50,51] Atomic force microscopy represented that the average diameter of CdTe NPs was measured as 3.7 nm within 10% standard deviation, and CdTe NWs have diameter of 5.8 ± 1.1 nm, average length of 1027 ± 92 nm (the aspect ratio of 179), and photoluminescence at 670 nm. Au NPs were synthesized based on the method of N. R. Jana et al.[52] In brief, a 20 mL aqueous solution containing $HAuCl_4$ of 2.5×10^{-4} M and trisodium citrate of 2.5×10^{-4} M was prepared in a conical flask. Next, 0.6 mL of ice-cold, freshly prepared 0.1 M $NaBH_4$ solution was added to the solution while stirring. The solution turned pink immediately after adding $NaBH_4$, indicating particle formation. The diameter of NPs was measured as 3.7 nm using transmission electron microscopy (TEM) images obtained with a JEOL 2010F transmission electron microscope.

To link affinity bioligands on Au NPs and CdTe NWs, a EDC/sulfo-NHS cross-linking procedure was utilized in both cases.[53] Fresh solutions of 0.2 M EDC, i.e., 0.07668 g of EDC in 2 mL of PBS buffer solution, and 25 mM NHS, i.e., 0.01085 g of NHS in 2 mL of PBS, were respectively prepared at pH 7.2. Boron (5 mg) was dissolved in 1 mL of PBS. The solutions of EDC, NHS, and B in the amounts of 1 mL each were mixed together with gentle stirring for 30 min at room temperature. A 2 mL portion of cysteine-stabilized CdTe NW dispersion was added into the resulting mixture and left to react for 2 h at room temperature with gentle stirring. The solution was stored at 4 °C and showed strong fluorescence for 2 weeks. The above proportion was adjusted within one tenth range when precipitation was observed in bioconjugated solution due to aggregation with NWs and biomolecules.

The procedure of bioconjugating Au NPs with SA was as follows. 10 mL of Au NP dispersion, 0.087 mmol of $HS(CH_2)_2CH_3$, and 0.272 mmol of $HS(CH_2)_2COOH$ were mixed for 24 h with stirring. EDC and NHS were reacted with this solution for 30 min. To this was added 1 mL of SA with a concentration of 1 mg/1 mL and left to react for 2 h.

The luminescence spectra of NP−NW dispersions were registered with a Fluoromax-3 spectrofluorometer made by Jobin Yvon/SPEX Horiba every 2−10 min for up to 2 h with continuous gentle stirring. The fluorescence lifetimes (τ) were measured with a Fluorolog Tau-3 (Jobin Yvon/SPEX Horiba) module of the Fluoromax-3 spectrofluorometer. The lifetime was measured from the 5−6 phase-modulation experiments under the same conditions. A sample with the dispersed NP−NW complex was extracted at the 30 min point after the beginning of the conjugation reaction, then the lifetime experiment was conducted for 10−20 min depending on the accuracy effort. The reference curves were collected for LUDOX TM-40, a colloidal silica 40 wt % suspension in water (Sigma, Saint Louis, MO), which is recommended by SPEX as a standard sample in lifetime measurements.

3. Results. The reaction of self-organization of CdTe NPs in CdTe NWs discovered recently[51] lends itself to the production of NW bioconjugates. In addition to high monodispersity of NW diameters, the reaction takes place in water, which greatly facilitates subsequent bioconjugation reactions. Aqueous media prevents coagulation and denaturation of proteins and eliminates the step of coating of NPs with organic or inorganic layers, rendering them water soluble.[18,21,54,55] Bioconjugation techniques typically involve DNA hybridization, antigen−antibody interactions, and ligand−receptor interactions, such as streptavidin (SA)−biotin (B).[49,56−58] The SA−B bond is known to be one of the strongest noncovalent methods of binding. The dissociation constant (K) of the complex between streptavidin and biotin is estimated at approximately 10^{-15} M.[59] Additionally, it was selected for this work because SA+B reaction is relatively fast and only marginally affected by pH, temperature, organic solvents, or other denaturing agents[60] that can be found in NP and NW dispersions.

NP−NW superstructures were obtained by mixing appropriate volumes of stock solutions of NP−SA and NW−B acting as elemental building blocks (see Experimental Section). This route is simple, easily scalable to volumes as small as nanoliters, and affords variation in the molar ratio between CdTe NWs and Au NPs. Both of these factors are important for the assembly processes carried out in microfluidics setups.

Table 1. Composition of Different NW+NP Complexes Prepared for Different Volume Ratios of the Stock NW−B and NP−SA Dispersions

	solution A	solution B	solution C	solution D
volume ratios, μL (CdTe NW:/Au NP)	20:10	20:20	20:30	20:40
NP/NW ratios	560	1100	1700	2250

The prepared CdTe NW−B dispersion was diluted four times to obtain a NW concentration of 4.0×10^{-9} mol. The molar concentration of NW was calculated with respect to NW 5.8 ± 1.1 nm in diameter with an average length of 1027 ± 92 nm. The Au NP−SA dispersion had molar concentration of 4.5×10^{-6} mol calculated assuming that the diameter of Au NPs is equal to 3.7 ± 0.3 nm. The reaction of NP−NW formation took place in 3 mL of water at pH 9 (pH adjusted with 0.1 M NaOH) in a quartz optical cuvette suitable for fluorescence spectroscopic investigations. Au NP dispersion was added to the cuvette in aliquots of 10∼40 μL, while the added volume of CdTe NW dispersion was constant and equal to 20 μL. For 1:1 volume ratio, i.e., 20 μL NW−B + 20 μL NP−S, it was calculated that approximately 1100 of Au NPs are bioconjugated to the surface of CdTe NWs. These calculations are based on two simple hypotheses: (1) all CdTe NPs used in the synthesis of CdTe NWs are transformed into NWs and (2) all Au NPs added to the dispersion are attached to the surfaces of CdTe NWs. Table 1 presents the calculated molar ratios of NPs and NWs in prepared complexes.

To gain insight into the structure of the prepared NP−NW hybrids, TEM images of unconjugated NWs and the colloids halfway through the bioconjugation reactions have been obtained (Figure 1A, B). Figure 1A presents a CdTe NW at relatively low magnification. No remaining original CdTe NPs can be observed. When Au NPs are conjugated to NWs (Figure 1B), they can be distinguished by the specific crystal lattice fringes of Au. From the HRTEM examination, the lattice parameter (*d* spacing) of the crystalline CdTe NWs was found to have lattice plane spacing of 0.398 ± 0.01 nm, which is typical for *hkl* (100) hexagonal wurtzite CdTe structures.[51] The Au NPs had a lattice spacing of 0.23 ± 0.008 nm, which corresponds to the (111) planes of Au crystal. From these images, one can clearly see that the NPs become attached to the CdTe surface. For longer conjugation time and for larger Au NPs amounts, dense layers of NPs were observed around the NWs. They were difficult to analyze by TEM due to overlapping diffraction patterns and strong electron scattering.

When NP−SA are added to NW−B, a distinct change in luminescence intensity of the CdTe nanocolloid can be seen (Figure 1D). Emission of band gap intensity of CdTe wires substantially increases in the course of conjugation and reaches the plateau in 65 min. The peak luminescence intensity was enhanced five times, while the maximum wavelength of each spectrum gradually shifted toward high energies (blue shift). Previously, an increase of the CdTe NP emission was observed when they become covalently conjugated to bovine serum albumin (BSA), which was attributed to the resonance energy transfer from BSA to

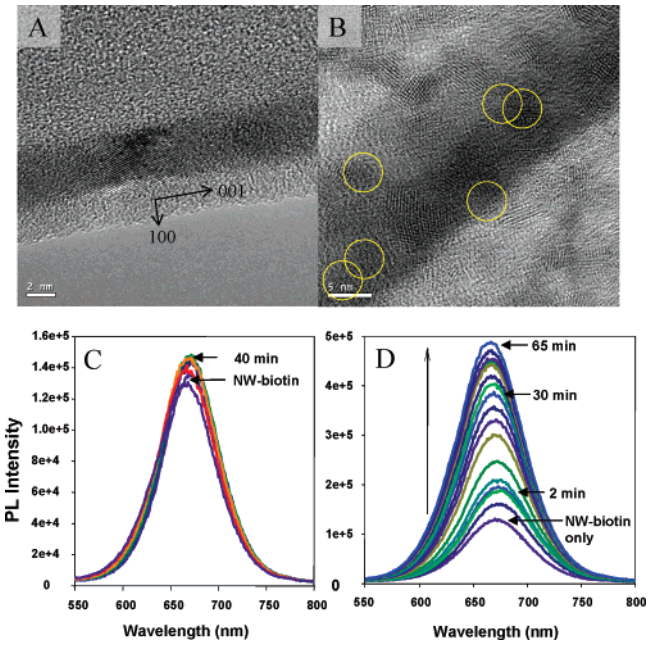

Figure 1. (A, B) TEM images of Au bioconjugated CdTe NW in solution B. (A) ×200 k, (B) ×500 k. Yellow circles indicate the areas where characteristic lattice fringes of 0.23 nm of (111) faces of metallic Au can be seen after bioconjugation. (C, D) Transient luminescence spectra of bioconjugated NWs in solution B. (C) NW−B with SA (without Au) monitored for 40 min after mixing, (D) NW−B with SA-Au monitored for 65 min. Excitation wavelength for both (C) and (D) is 420 nm.

CdTe.[53] However, this effect does not occur here. When only SA solution is added to NW−B, no significant change in the luminescence intensity or emission spectrum can be seen (Figure 1C) because the excitation wavelength does not excite the aromatic and other amino acid moieties of SA.

The increase in luminescence intensity of NW emission depends on the number of Au NPs added. This fact is reflected in Figure 2 as the dependence of luminescence on the molar ratio of CdTe NWs to Au NPs. One can see a steady increase in the ultimate fluorescence intensity after 20 min of bioconjugation as the average number of Au NPs adsorbed on a NW increased from 560 (Figure 2A) to 2250 (Figure 2D). It is also important to note the tendency of the luminescence to saturate after about 30 min for all of the NP/NW ratios. This time correlates well with the expected kinetics of SA−B bonding in bioconjugation reactions involving nanocolloids.[46]

The dependence of the luminescence intensity on the amount of attached NPs as well as the spectral shift of NW emission indicated to us that these optical effects are likely to be related to the interaction of plasmons in Au NPs and excitons in NWs. To provide adequate experimental verification of this model (see Discussion), the interplay between the luminescence lifetime (τ), luminescence enhancement, and the blue shift of emission spectrum was monitored (Figure 3A). Interestingly, as the luminescence increases, the PL lifetime gradually decreases. This is contrary to classical observations in luminescence quenching and activation when emission enhancement is accompanied by longer lifetimes.[61] This illustrates the difference in photophysics of interacting

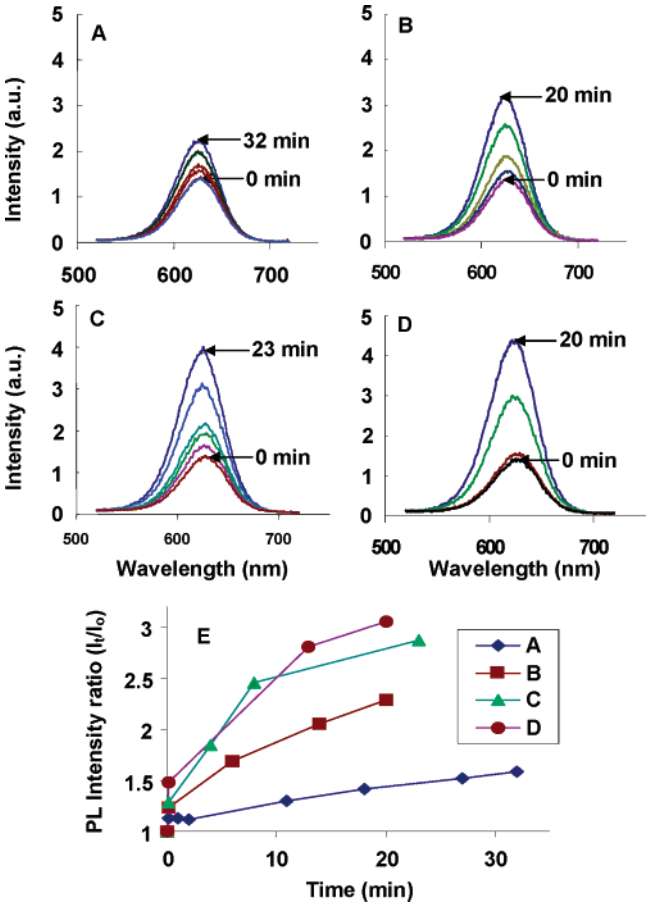

Figure 2. (A−D) Transient luminescence spectra of CdTe NWs for different molar ratios of CdTe NWs to Au NPs. NP/NW is equal to 560, 1100, 1700, and 2250 for (A), (B), (C), and (D), respectively. Condition of PL registration and the range of PL intensities for graphs (A−D) PL intensity are identical. (E) Comparative time courses of the peak intensities for the same experiments.

nanocolloids and organic fluorophores. At this point, one can also suspect that the nature of the optical effects here is related to the interaction of excitons in the NWs and surface plasmons in Au NPs,[62] which will be discussed in detail below. Before the theoretical considerations though, it is important to establish the reversible nature of the luminescence enhancement taking place when the NP−NW bioconjugated superstructure is forming. This is necessary to eliminate possible artifacts unrelated to SA−B reactions and stemming from some accidental impurities. As well, the reversibility of the optical enhancement can open the door for the design of various biosensors based on this phenomenon.

To induce the reverse reaction, i.e., separation of the NP−NW superstructure, an excess amount of unconjugated SA was added to the dispersion. Addition of extra SA shifts the equilibrium in SA + B → SA−B reaction and results in the disruption of some of bonds between bioconjugated CdTe NWs and Au NPs. The reverse process can also be described as competitive replacement of the NP-conjugated SA molecule with an unconjugated one.[63,64] The concentration of extra SA added to the formed NP−NW superstructure was 0.8 mg in 0.2 mL PBS buffer, which was at least several thousand times higher than the concentration of SA in Au bioconjugates. As expected, once the SA was added the luminescence intensity decreased and the wavelength shifted to the red (Figure 3C). The characteristic time of the reaction, i.e., 20−30 min, correlates well with the original time of bioconjugate formation (Figure 2E) as well as with the expected time period necessary for the competitive replacement of one partner in the biological affinity pairs.[49,65,66] Notice that the reversal is not complete and the decrease of the luminescence stops somewhere halfway down to the original NW solution, which happens, most likely, due to strong van der Waals interactions between NPs and NWs.

The following phase-modulation lifetime experiments extended our understanding about the interaction of metallic and semiconducting nanomaterials. Figure 3A shows a gradual decline of lifetime when the NP−NW superstructure is forming, while the PL of CdTe NW is becoming stronger. Figure 3B shows that the addition of SA caused the definite elongation of lifetime D for the competitive replacement reaction reversing the formation of NP−NW superstructure. The physical significance of this observation is that it gives clear evidence that the observed enhancement of the luminescence is reversible, and therefore, the obtained supramolecule retains relevant characteristics of the original biomolecules. Besides the potential use of this effect in engineering of biosensors, these experiments unequivocally proved that the enhancement of PL and blue shift resulted from the conjugation of Au NP on CdTe NW.

4. Discussion. Luminescence enhancements in Au NP bioconjugated CdTe NW is reminiscent of surface enhanced Raman scattering (SERS) resulting from the electromagnetic enhancement of laser fields due to polarization of metal NPs.[34,67−70] Incident light illumination of the solution excites plasmons in the metal NPs. Plasmon excitations result in strong electromagnetic fields in the vicinity of Au NPs, which we believe might be the likely reason for the increase of optical emission of NWs from the conjugation with metallic NPs.

The total electric field, $\mathbf{E}_{tot}$, induced by the incident light nearby an Au NP can be calculated as

$$\mathbf{E}_{tot} = \mathbf{E}_{ext} + \frac{3\mathbf{n}(\mathbf{dn}) - \mathbf{d}}{\epsilon_0 R^3}$$

Here we assume that the center of coordinates is in the center of Au NP; $\mathbf{E}_{ext}$ and $\mathbf{d}$ are the external electric field and the induced dipole moment of Au NP; R and $\mathbf{n}$ are the distance to the center of NP and the unit vector directed from the center of NP. The dipole moment of a spherical NP is given by an equation:

$$\mathbf{d} = \epsilon_0 a^3 \frac{\epsilon_m(\omega) - \epsilon_0}{\epsilon_m(\omega) + 2\epsilon_0}\mathbf{E}_{ext}$$

where a is the radius and $\epsilon_m(\omega)$ and ϵ_0 are the dielectric constants of the metal and surrounding media.[71] Since the NPs and NWs in liquid are randomly oriented, the enhance-

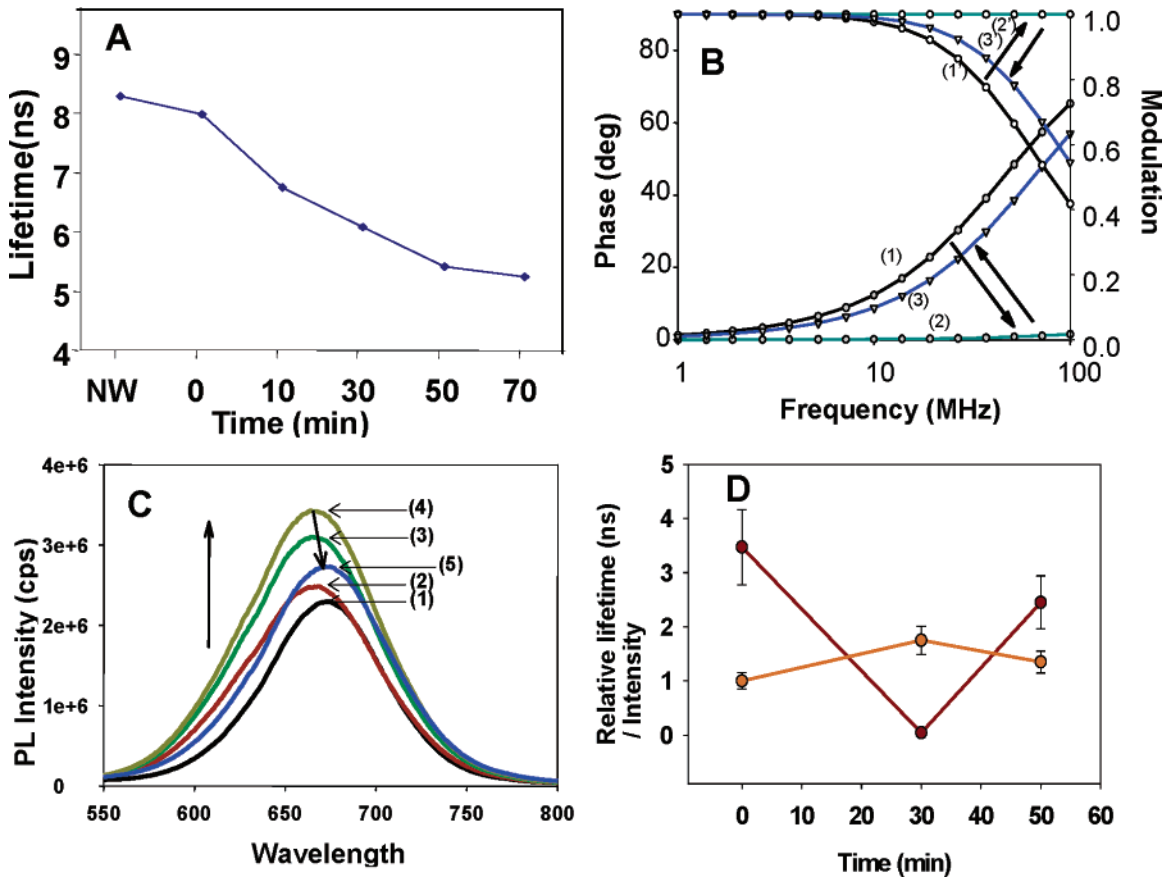

Figure 3. (A) Variation of the luminescence lifetime experiments during the formation of NP−NW superstructures in solution B. The time in the abscissa corresponds to the time after mixing of the NW−B and Au−SA solutions. Lifetime experiments were carried out for the samples identical in composition to those in Figure 1D. (B) Lifetime (τ) measurements of CdTe NWs luminescence bioconjugated with Au−SA for competitive replacement experiment (see graph D): (1) CdTe NW−B only, (2) Au bioconjugated NW for 30 min, and (3) 20 min later after adding extra SA; (1−3) are for phase mode, and (1′−3′) for modulation mode. (C) The reversibility of NW−B + Au−SA reaction and corresponding luminescence effects: (1) CdTe NW-biotin, (2) 10 min later after addition of Au−SA, (3) 20 min later, (4) 30 min later, and (5) 20 min after adding extra SA to (4). (D) Correlation between the relative lifetimes (τ) and luminescence intensities for the reactions of NP−NW superstructure formation and competitive replacement of SA. At the 30 min point excess of SA was added to the reaction mixture.

ment for the squared electric field should be averaged over solid angles Ω: $R(\omega) = \langle \mathbf{E}^2_{\mathrm{tot}} \rangle_\Omega / \langle \mathbf{E}^2_{\mathrm{ext}} \rangle_\Omega$. It is known that the plasmon excitations in Au NPs are strongly damped and the approximation for the dielectric constant can be presented in the form $\epsilon_{\mathrm{m}}(\omega) = 9 + 5i - (\omega_{\mathrm{p}}/\omega)^2$, where $\hbar\omega_{\mathrm{p}} = 8$ eV.[72] To make choice for the dielectric constant ϵ_0, we compared the experimental UV absorption spectrum of SA-B−Au NPs (see Supporting Information Figure 1) and the theoretical result for UV absorption. The experimental plasmon peak appears at 530 nm. We obtain the same plasmon peak frequency if we choose $\epsilon_0 = 1.8$. The above number for ϵ_0 describes an effective dielectric constant of organic molecules surrounding the Au NPs. Figure 4A shows the calculated enhancement factor $R(\lambda)$ in the center of the NW for the parameters $a = 1.85$ nm and $R = 9.75$ nm. Here, R is the typical distance between the center of NP and the central line of NW (for the sizes of NPs and SA-B molecules see Figure 5). The enhancement of fluorescence due to plasmons can come from the increase of incident electromagnetic field (at $\lambda_{\mathrm{laser}} = 420$ nm) or from the increase of radiative probability of NW excitons (at about 660 nm). We see from Figure 4A that the enhancement factor for the chosen distance R in the regions of the fluorescence peak ($\lambda_{\mathrm{emission}} = 660$ nm) and the laser wavelength (420 nm) is close to 1. Therefore, the electromagnetic enhancement coming from a single Au NP is almost absent. One physical reason for this is that the plasmon peak in Au−NPs is strongly broadened and hence the electron plasma of NPs represents an oscillator with a relatively low quality factor. Another reason is the relatively large NP−NW distance ($R \approx 10$ nm) in our bioconjugates.

We now estimate the enhancement factor for the superstructure formed by numerous Au NPs around a NW. To understand optical phenomena in NP−NW superstructures, it is convenient to use the ideal model of conjugate structures depicted in Figure 5. This cartoon is based on the assumptions of completeness of the reaction of NP→NW transition and the reaction of Au bioconjugation discussed above. Taking into consideration that the diameter of SA occupied by B is 5 nm[73−76] and that diameters of CdTe NWs and Au NPs are 5.8 ± 1.1 nm and 3.7 ± 0.3 nm, respectively, we can treat the system as closely packed NPs around the NW (Figure 5). The NP/NW molar ratio necessary for this arrangement is 2250, which corresponds to solution D.

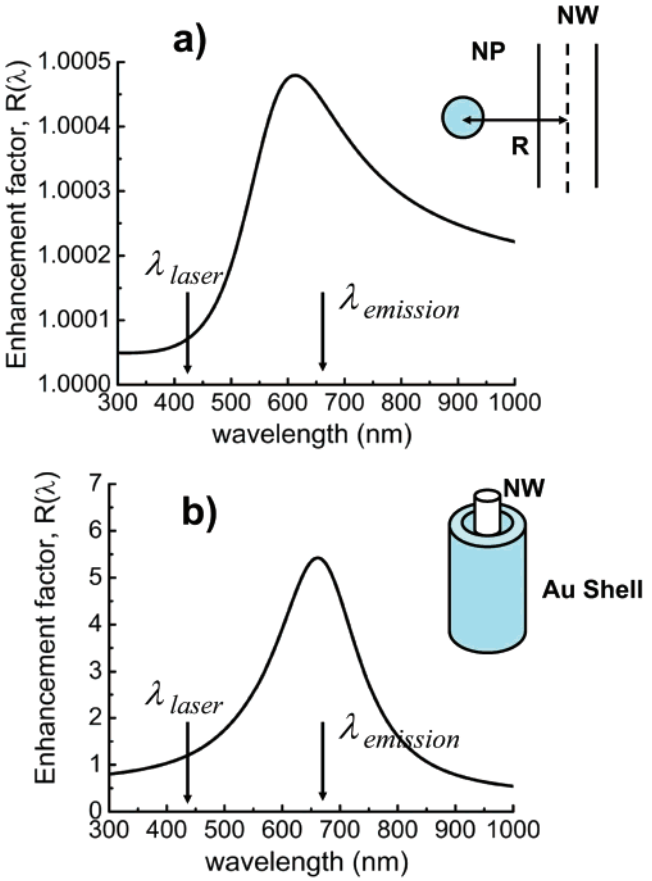

Figure 4. (A) Calculated electric-field enhancement factor as a function of the wavelength of light in the center of NW in the presence of a single conjugated Au−NP. (B) Calculated enhancement factor as a function of the wavelength of light in the center of a cylindrical shell made of Au. Arrows show the wavelengths related to the incident light and fluorescence peak. Note different scales for the enhancement factor in figures (a) and (b). Insets represent geometry of the systems.

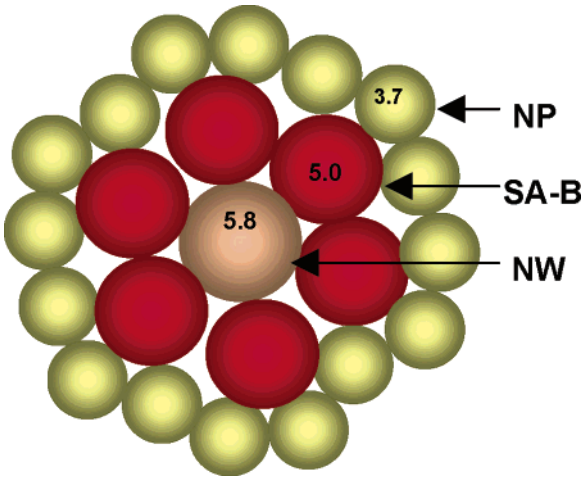

Figure 5. Cross section of closely packed model arrangement of CdTe NW and Au NP in the bioconjugate.

The NP system around the central CdTe NW can be viewed as a shell. Therefore, as a second model, we now consider a cylindrical shell made of Au (Figure 4B, inset). This model describes the limiting case when the Au NPs cover the entire surface of NW and respond to the incident electromagnetic field collectively. In this approach we neglect the discreteness of the NP shell, which can, in principle, be a source of an additional enhancement of electromagnetic field. Despite these shortcomings, this model allows us to describe the collective response of strongly interacting NPs. The collective character of the response is practically important since the electric field enhancement factor can increase the efficiency of laser devices and expand the working range of NP sensors. It has also obvious importance from the fundamental points of view as a demonstration of special properties of nanoscale superstructures assembled from individual NPs.

The electric field inside of the cylindrical shell in the long wavelength limit can be presented as $\mathbf{E}_{\text{tot},\parallel} = \mathbf{E}_{\text{ext},\parallel}$ and $\mathbf{E}_{\text{tot},\perp} = \mathbf{E}_{\text{ext},\perp} f(\omega)$, where $\mathbf{E}_\perp$ ($\mathbf{E}_\parallel$) are the field components perpendicular (parallel) to the NW; the function $f(\omega) = 4\gamma(\omega)/[(\gamma(\omega) + 1)^2 - (\gamma(\omega) - 1)^2(R_{\text{in}}/R_{\text{out}})^2]$, $\gamma(\omega) = \epsilon_{\text{m}}(\omega)/\epsilon_0$, and $R_{\text{in}}(R_{\text{out}})$ are the inner (external) radii of the Au-shell.[71] Taking $R_{\text{in}} = 7.9$ nm and $R_{\text{out}} = 11.6$ nm and averaging the field over solid angles, we calculate the field enhancement factor, $R(\omega) = \langle \mathbf{E}_{\text{tot}}^2 \rangle_\Omega / \langle \mathbf{E}_{\text{ext}}^2 \rangle_\Omega$ (Figure 4B). The above values for $R_{\text{in(out)}}$ correspond to the virtual arrangement shown in Figure 5. We can see a remarkable enhancement of electric fields at $\lambda \approx 600$ nm in Figure 4B. As it was pointed out, the enhancement of fluorescence may come from either the process of absorption of an incident photon or the process of emission of a secondary photon. Therefore, we have to examine the factor $R(\omega_{\text{laser}})R(\omega_{\text{emission}})$, where $\omega_{\text{laser}}(\omega_{\text{emission}})$ is the frequency of incident (re-emitted) photons. For the wavelengths from our experiments, the calculated enhancement factor $R(\omega_{\text{laser}})R(\omega_{\text{emission}}) \approx 6.5$. Since the peak position in Figure 4B is close to the position of the fluorescence peak ($\lambda_{\text{emission}} = 660$ nm), the main contribution to the calculated enhancement factor $R(\omega_{\text{laser}})R(\omega_{\text{emission}})$ comes from the increase of emission probability, which correlates very well with the fact that the lifetimes of the NWs after conjugations are substantially shortened. The calculated enhancement factor for the shell model is close to the experimental factor of 5, which coincides with the observed experimental value amazingly well. Note that in this model we assume that the NPs are tightly packed to form a shell. In real conjugated NWs, the Au−NPs may densely cover the surface of the NW, although not being as tightly packed as in Figure 5. Our theoretical results for the enhancement factor look very reasonable, especially considering the fact that the cylindrical shell model represents the limiting case for NP−NW superstructure geometry. It is important to emphasize that, according to the above argument, this model can provide only a semi-quantitative description of the experiments. Moreover, several other factors can contribute to the enhancement: the decrease of nonradiative lifetime of exciton in the presence of Au NPs[64] (1), the discreteness of NPs (2), and the randomness of NP positions (3). The first factor should reduce the enhancement coefficient. The second can increase the electromagnetic enhancement since almost any type of deviation from the simplest geometries results in local enhancement of electromagnetic fields.[70−74] Regarding the third factor, it is known from SERS and previous

experiments on photoluminescence that the random fields induced by a rough metallic surface result in a strong electric field enhancement.[70] Thus this degree of disorder in bioconjugate can be another factor leading to the enhancement of fluorescence. According to the results obtained within the two models described, one can conclude that the plasmon-induced enhancement of electric fields can originate from collective excitations in a system of interacting Au NPs. Single, noninteracting Au NPs cannot provide any enhancement. In contrast, single Au−NPs will likely lead to a suppression of fluorescence due to an increase of nonradiative losses.[62]

As it was mentioned above, the two experimental facts (the strong fluorescence enhancement and the lifetime shortening) nicely correlate with each other. The inverse lifetime of exciton is composed of two terms: $1/\tau = \gamma_{rad} + \gamma_{non-rad}$, where $\gamma_{rad}(\gamma_{non-rad})$ are the radiative and nonradiative rates, respectively. The radiative rate $\gamma_{rad} \propto R(\omega)$ and increases with the field enhancement factor; this is due to the effective local density of states of photons.[77] The above argument naturally explains the observed correlation between the emission intensity and lifetime.

Experimental observations in Figures 2A−D and 3C related to the blue shift of the NP conjugate can also be explained very well on the basis of exciton−plasmon interactions. In the presence of Au−NPs, the lifetime of excitons becomes shorter and consequently the diffusion length of excitons in a NW decreases. Since the NW is not entirely homogeneous and has some variations in the structure and diameter along the NW length, short-lived excitons do not have enough time to diffuse into the regions of the NWs with the lowest energies and therefore create photons in the regions of the NWs with relatively large band gap. Consequently, the population of the comparatively narrow band-gap regions decreases and the emission is observed from the places close to the point of their absorption. This is consistent with the blue shift in the luminescence spectra of the NW−NP superstructures, which was also observed in other related systems.[70]

5. Conclusion. SA-B affinity in NW and NP bioconjugates was used to form a new type of NP−NW superstructure. Au−NPs form dense granular coatings around the luminescent CdTe NWs, which results in unique optical effects stemming from exciton−plasmon interactions. The peak luminescence intensity of NW increased as much as five times with Au NPs in the course of the bioconjugation reaction. In addition, the blue shift of CdTe NW light emission and substantial shortening of the luminescence lifetime were observed. It is suggested that the electromagnetic enhancement from polarized Au NPs in the vicinity of CdTe NWs is the reason of the luminescence enhancement and related effects. Using a simple theoretical model, we demonstrate that the origin of the strong enhancement effect is a collective response of an ensemble of interacting Au NPs.

Supporting Information Available: Supplementary Figure 1: Absorbance of Au−NP and SA-conjugated NPs. This material is available free of charge via the Internet at http://pubs.acs.org.

References

(1) Redl, F. X.; Cho, K. S.; Murray, C. B.; O'Brien, S. *Nature (London)* **2003**, *423*, 968−971.
(2) Hoertz, P. G.; Carlisle, R. A.; Meyer, G. J.; Wang, D.; Piotrowiak, P.; Galoppini, E. *Nano Lett.* **2003**, *3*, 325−330.
(3) Zhang, Q. F.; Liu, W. M.; Xue, Z. Q.; Wu, J. L.; Wang, S. F.; Wang, D. L.; Gong, Q. H. *Appl. Phys. Lett.* **2003**, *82*, 958−960.
(4) Zhang, J.; Coombs, N.; Kumacheva, E.; Lin, Y.; Sargent, E. H. *Adv. Mater.* **2002**, *14*, 1756−1759.
(5) Galoppini, E.; Guo, W.; Zhang, W.; Hoertz, P. G.; Qu, P.; Meyer, G. J. *J. Am. Chem. Soc.* **2002**, *124*, 7801−7811.
(6) Shipway, A. N.; Willner, I. *Chem. Commun.* **2001**, 2035−2045.
(7) Kulakovich, O.; Strekal, N.; Yaroshevich, A.; Maskevich, S.; Gaponenko, S.; Nabiev, I.; Woggon, U.; Artemyev, M. *Nano Lett.* **2002**, *2*, 1449−1452.
(8) Benson, D. E.; Conrad, D. W.; de Lorimier, R. M.; Trammell, S. A.; Hellinga, H. W. *Science* **2001**, *293*, 1641−1644.
(9) Alivisatos, A. P.; Johnsson, K. P.; Peng, X.; Wilson, T. E.; Loweth, C. J.; Bruchez, M. P., Jr.; Schultz, P. G. *Nature (London)* **1996**, *382*, 609−611.
(10) Jin, R.; Wu, G.; Li, Z.; Mirkin, C. A.; Schatz, G. C. *J. Am. Chem. Soc.* **2003**, *125*, 1643−1654.
(11) Parak, W. J.; Pellegrino, T.; Micheel, C. M.; Gerion, D.; Williams, S. C.; Alivisatos, A. P. *Nano Lett.* **2003**, *3*, 33−36.
(12) Storhoff, J. J.; Elghanian, R.; Mirkin, C. A.; Letsinger, R. L. *Langmuir* **2002**, *18*, 6666−6670.
(13) Nam, J. M.; Stoeva, S. I.; Mirkin, C. A. *J. Am. Chem. Soc.* **2004**, *126*, 5932−5933.
(14) Kraemer, S.; Xie, H.; Gaff, J.; Williamson, J. R.; Tkachenko, A. G.; Nouri, N.; Feldheim, D. A.; Feldheim, D. L. *J. Am. Chem. Soc.* **2004**, *126*, 5388−5395.
(15) Harnack, O.; Ford, W. E.; Yasuda, A.; Wessels, J. M. *Nano Lett.* **2002**, *2*, 919−923.
(16) Zanchet, D.; Micheel, C. M.; Parak, W. J.; Gerion, D.; Williams, S. C.; Alivisatos, A. P. *J. Phys. Chem. B* **2002**, *106*, 11758−11763.
(17) Bielinska, A.; Eichman, J. D.; Lee, I.; Baker, J. R., Jr.; Balogh, L. *J. Nanopart. Res.* **2002**, *4*, 395−403.
(18) Bruchez, M., Jr.; Moronne, M.; Gin, P.; Weiss, S.; Alivisatos, A. P. *Science* **1998**, *281*, 2013−2016.
(19) Katz, E.; Willner, I.; Wang, J. *Electroanalysis* **2004**, *16*, 19−44.
(20) Zhang, H.; Lee, K. B.; Li, Z.; Mirkin, C. A. *Nanotechnology* **2003**, *14*, 1113−1117.
(21) Dubertret, B.; Skourides, P.; Norris, D. J.; Noireaux, V.; Brivanlou, A. H.; Libchaber, A. *Science* **2002**, *298*, 1759−1762.
(22) Kotov, N. A. *Bioconjugates of nanoparticles as radiopharmaceuticals*; The Board of Regents for Oklahoma State University; 2001-US17658(2001091808), 26-20011206. WO. 5-31-2001.
(23) West, J. L., Halas, N. J., Oldenburg, S. J., Averitt, R. D. *Metal nanoshells for biosensing applications*; Wm. Marsh Rice University, 2000-616154(6699724), 20-20040302. 2004. US. 7-14-2000.
(24) Cao, Y. C.; Jin, R.; Mirkin, C. A. *Science* **2002**, *297*, 1536−1540.
(25) Nam, J.; Thaxton, C. S.; Mirkin, C. A. *Science* **2003**, *301*, 1884−1886.
(26) Sinani, V. A.; Koktysh, D. S.; Yun, B.-G. Matts, R. L.; Pappas, T. C.; Motamedi, M.; Thomas, S. T.; Kotov, N. A. *Nano Lett.* **2003**, *3*, 1177−1182.
(27) Bulka, B. R.; Stefanski, P. *Phys. Rev. Lett.* **2001**, *86*, 5128−5131.
(28) Lee, Y. H.; Kim, D. H.; Shin, K. S.; Choi, C. H.; Jang, Y. T.; Ju, B. K. *Appl. Phys. Lett.* **2003**, *82*, 3535−3537.
(29) Hung, C. H.; Whang, W. T. *Mater. Chem. Phys.* **2003**, *82*, 705−710.
(30) Kim, H. M.; Kang, T. W.; Chung, K. S. *Adv. Mater.* **2003**, *15*, 567−569.
(31) Zhang, Y.; Ichihashi, T.; Landree, E.; Nihey, F.; Iijima, S. *Science* **1999**, *285*, 1719−1722.
(32) Pileni, M. P.; Lalatonne, Y.; Ingert, D.; Lisiecki, I.; Courty, A. *Faraday Discuss.* **2003**, *125*, 251−264.
(33) Brust, M.; Kiely, C. J. *Colloids Surf., A* **2002**, *202*, 175−186.
(34) Vo-Dinh, T. *TrAC, Trends Anal. Chem.* **1998**, *17*, 557−582.
(35) Thomas, K. G.; Kamat, P. V. *Acc. Chem. Res.* **2003**, *36*, 888−898.
(36) Link, S.; El Sayed, M. A. *Ann. Rev. Phys. Chem.* **2003**, *54*, 331−366.
(37) Willner, I.; Willner, B. *Pure Appl. Chem.* **2002**, *74*, 1773−1783.

(38) Shipway, A. N.; Katz, E.; Willner, I. *ChemPhysChem* **2000**, *1*, 18−52.
(39) Carrillo, A.; Swartz, J. A.; Gamba, J. M.; Kane, R. S.; Chakrapani, N.; Wei, B.; Ajayan, P. M. *Nano Lett.* **2003**, *3*, 1437−1440.
(40) Ravindran, S.; Bozhilov, K. N.; Ozkan, C. S. *Carbon* **2004**, *42*, 1537−1542.
(41) Liu, L.; Wang, T.; Li, J.; Guo, Z. X.; Dai, L.; Zhang, D.; Zhu, D. *Chem. Phys. Lett.* **2002**, *367*, 747−752.
(42) Larciprete, R.; Lizzit, S.; Botti, S.; Cepek, C.; Goldoni, A. *Phys. Rev. B* **2002**, *66*, 121402.
(43) Homma, Y.; Yamashita, T.; Kobayashi, Y.; Ogino, T. *Physica B* **2002**, *323*, 122−123.
(44) Ajayan, P. M.; Iijima, S. *Nature (London)* **1993**, *361*, 333−334.
(45) Osterloh, F. E.; Martino, J. S.; Hiramatsu, H.; Hewitt, D. P. *Nano Lett.* **2003**, *3*, 125−129.
(46) Penner, R. M. *J. Phys. Chem. B* **2002**, *106*, 3339−3353.
(47) Parak, W. J.; Gerion, D.; Zanchet, D.; Woerz, A. S.; Pellegrino, T.; Micheel, C.; Williams, S. C.; Seitz, M.; Bruehl, R. E.; Bryant, Z.; Bustamante, C.; Bertozzi, C. R.; Alivisatos, A. P. *Chem. Mater.* **2002**, *14*, 2113−2119.
(48) Maxwell, D. J.; Taylor, J. R.; Nie, S. *J. Am. Chem. Soc.* **2002**, *124*, 9606−9612.
(49) Wang, S.; Mamedova, N.; Kotov, N. A.; Chen, W.; Studer, J. *Nano Lett.* **2002**, *2*, 817−822.
(50) Gaponik, N.; Talapin, D. V.; Rogach, A. L.; Hoppe, K.; Shevchenko, E. V.; Kornowski, A.; Eychmueller, A.; Weller, H. *J. Phys. Chem. B* **2002**, *106*, 7177−7185.
(51) Tang, Z.; Kotov, N. A.; Giersig, M. *Science* **2002**, *297*, 237−240.
(52) Jana, N. R.; Gearheart, L.; Murphy, C. J. *Langmuir* **2001**, *17*, 6782−6786.
(53) Mamedova, N. N.; Kotov, N. A.; Rogach, A. L.; Studer, J. *Nano Lett.* **2001**, *1*, 281−286.
(54) Nie, S. *Water-soluble luminescent quantum dots and biomolecular conjugates thereof and related compositions and methods of use*; Advanced Research and Technology Institute, Inc. USA. 99-US21793(2000029617), 45-20000525. WO. 9-24-1999.
(55) Shavel, A.; Gaponik, N.; Eychmueller, A. *J. Phys. Chem. B* **2004**, *108*, 5905−5908.
(56) Hai, X.; Tan, M.; Wang, G.; Ye, Z.; Yuan, J.; Matsumoto, K. *Anal. Sci.* **2004**, *20*, 245−246.
(57) Ye, Z.; Tan, M.; Wang, G.; Yuan, J. *J. Mater. Chem.* **2004**, *14*, 851−856.
(58) Zhao, X.; Tapec-Dytioco, R.; Tan, W. *J. Am. Chem. Soc.* **2003**, *125*, 11474−11475.
(59) Sano, T.; Vajda, S.; Cantor, C. R. *J. Chromatogr. B* **1998**, *715*, 85−91.
(60) Gref, R.; Couvreur, P.; Barratt, G.; Mysiakine, E. *Biomaterials* **2003**, *24*, 4529−4537.
(61) Turro, N. J. *Modern Molecular Photochemistry*; Benjamin/Cummings: Menlo Park, CA, 1978; p 628.
(62) Dulkeith, E.; Morteani, A. C.; Niedereichholz, T.; Klar, T. A.; Feldmann, J.; Levi, S. A.; van Veggel, F. C. J. M.; Reinhoudt, D. N.; Moller, M.; Gittins, D. I. *Phys, Rev. Lett.* **2002**, *89*, 203002.
(63) Biswal, S. L.; Gast, A. P. *Phys. Rev. E* **2003**, *68*, 021402.
(64) Shimoboji, T.; Ding, Z.; Stayton, P. S.; Hoffman, A. S. *Bioconjugate Chem.* **2001**, *12*, 314−319.
(65) Williams, E.; Pividori, M. I.; Merkoci, A.; Forster, R. J.; Alegret, S. *Biosens. Bioelectron.* **2003**, *19*, 165−175.
(66) Patel, A. B.; Allen, S.; Davies, M. C.; Roberts, C. J.; Tendler, S. J. B.; Williams, P. M. *J. Am. Chem. Soc.* **2004**, *126*, 1318−1319.
(67) Moskovits, M.; Tay, L. L.; Yang, J.; Haslett, T. *Top. Appl. Phys.* **2002**, *82*, 215−226.
(68) Jensen, T.; Kelly, L.; Lazarides, A.; Schatz, G. C. *J. Cluster Sci.* **1999**, *10*, 295−317.
(69) Quinten, M. *Appl. Phys. B* **2001**, *73*, 245−255.
(70) Shimizu, K. T.; Woo, W. K.; Fisher, B. R.; Eisler, H. J.; Bawendi, M. G. *Phys. Rev. Lett.* **2002**, *89*, 117401.
(71) Landau, L. D. *Electrodynamics of Continuous Media*, Translated from the Russian by J. Sykes and J. S. Bell; Oxford: New York, 1960; p 413.
(72) Aizpurua, J.; Hanarp, P.; Sutherland, D. S.; Kall, M.; Bryant, G. W.; Garcia de Abajo, F. J. *Phys. Rev. Lett.* **2003**, *90*, 057401.
(73) Yan, H.; Park, S. H.; Finkelstein, G.; Reif, J. H.; LaBean, T. H. *Science* **2003**, *301*, 1882−1884.
(74) Li, M.; Mann, S. *J. Mater. Chem.* **2004**, *14*, 2260−2263.
(75) Kaplan, D. L.; Davey, M. J.; O'Donnell, M. *J. Biol. Chem.* **2003**, *278*, 49171−49182.
(76) Shin, J. H.; Jiang, Y.; Grabowski, B.; Hurwitz, J.; Kelman, Z. *J. Biol. Chem.* **2003**, *278*, 49053−49062.
(77) Vogel, W.; Welsch, D. G.; Wallentowitz, S.; Editors. *Quantum Optics: An Introduction*, 2nd enlarged edition; 2000; p 480.

NL048669H